

DETECTING GROUND SETTLEMENT OF SHANGHAI USING INTERFEROMETRIC SYNTHETIC APERTURE RADAR (INSAR) TECHNIQUES

P. Damoah-Afari^{a,*}, X.L. Ding^a, Z. Lu^b, Z.W. Li^c

^a The Hong Kong Polytechnic University, Hung Hom, Kowloon, Hong Kong - (p.damoah, lsxlding)@polyu.edu.hk

^b U.S. Geological Survey, Vancouver, Washington, USA - lu@usgs.gov

^c Central South University, Changsha 410083, Hunan, China - zwli@mail.csu.edu.cn

Commission VII, WG VII/2

KEY WORDS: Hazard Mapping, Land Subsidence, Deformation Analysis, SAR, InSAR, DInSAR, PSInSAR

ABSTRACT:

Differential (D) and persistent scatterer (PS) interferometric synthetic aperture radar (InSAR) (DInSAR and PSInSAR) techniques are arguably the most cost effective and efficient methods today for ground surface deformation monitoring since their invention in the last quarter of the twentieth century. They overcome the limitations of traditional methods of deformation monitoring with regards to cost, time, man power and environmental conditions. A study has been conducted using the above techniques to investigate the land subsidence phenomena in Shanghai. Data from both the European Remote Sensing (ERS) Satellite 1 and 2 (ERS-1/2) and the Japanese Earth Resource Satellite 1 (JERS-1) were used. Results of ground surface subsidence using (i) the DInSAR technique with the L-band JERS-1 SAR data, and (ii) the PSInSAR technique with the C-band ERS-1/2, have been produced for Shanghai. Consistent deformation rates for each dataset used have been produced using the DInSAR and the PSInSAR techniques. Qualitative analysis of the differential interferograms produced from L-band JERS-1 SAR data yields a more accurate and consistent land subsidence pattern in Shanghai. Three stages of land subsidence are revealed by a series of L-band JERS-1 differential interferograms covering Shanghai from 1992-1998. The results obtained from PSInSAR processing, although a bit noisy, are also in agreement with both the results obtained from the DInSAR processing, and land subsidence map of Shanghai produced from other survey techniques.

1. INTRODUCTION

1.1 Land Subsidence in Shanghai

The city of Shanghai has been experiencing land subsidence mainly due to anthropogenic induced factors such as intensive exploitation of ground water (Shi and Bao, 1984; Zhang et al., 2002; China Daily, 2003a; 2003b; Chai et al., 2004; Hu et al., 2004; Damoah-Afari et al., 2005; Xue et al. 2005), and the massive construction of high-rise buildings in the downtown area (Zhang et al., 2002; China Daily, 2003a; 2003b; Xue et al. 2005; Zhang and Wei, 2005; Gong et al., 2005). It is estimated that the concentration of high-rise buildings in the downtown area contribute about 30 to 40 per cent of the subsidence problem. Results of dynamic monitoring have indicated that, the city centre subsided by 36mm between 1986 and 1990, 53.8mm between 1991 and 1995, and 98.8mm between 1996 and 2000 (Zhang and Wei, 2005).

According to Shi and Bao (1984), the problem of land subsidence in Shanghai was first reported in 1921, and the problem continued till 1963 when its impact became more severe. A cumulative subsidence of 2.63m was observed with greatest subsidence occurring between 1956 and 1959, at an annual rate of 98mm. In 1963, some measures such as restriction and rational usage of ground water, artificial recharge of ground water, and adjustment of exploited aquifers (Shi and Bao, 1984; Deng and Ju, 1994), were put in place to check the subsidence problem. The enforcement of those measures resulted in considerable rebound of water level

between 1966 and 1971. The Shanghai Municipal Government in 1995 came out with another policy that limited the usage of underground water of the whole city to less than 10 million cubic meters per year, and also demanded that all deep wells in the city are to operate with official permits (China Daily, 2003a; Xue et al., 2005). The historical development of land subsidence in Shanghai at 6 epochs during the period 1921-2000, is provided in Figure 1.

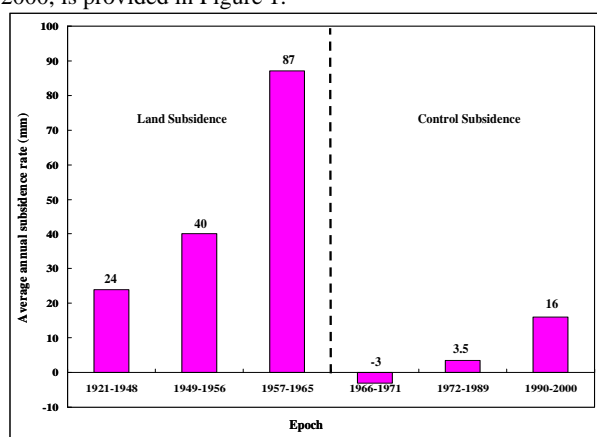


Figure 1. Historical development of land subsidence in Shanghai from 1921-2000 (Source: Zhang et al., 2002).

In spite of these measures, Shanghai is still experiencing some degree of subsidence (China Daily, 2003a; Xue et al., 2005).

* Corresponding author

The average land subsidence rates, gathered from Shanghai Geological Survey Institute, are 12.12 mm in 2000, 10.94 mm in 2001, and 10.22 mm in 2002 (China Daily, 2003a), and the target land subsidence rates as perceived by the Shanghai Municipal Land and Resources Administration Bureau are at most 10 mm by 2005 and 5mm by 2010 (Zhang and Wei, 2005).

Subsidence phenomenon in Shanghai has been previously measured or monitored using the surveyor’s method of precise levelling, and more recently the GPS. Although these methods provide precise measurements they are labour and time intensive, costly and are restricted to specific points in the terrain. They cannot therefore be used to provide information on detailed ground motions if the area of ground subsidence is large. Interferometric synthetic aperture radar (InSAR), a space geodetic method, has demonstrated the capability of mapping extensive areas, on pixel-by-pixel basis, and in a more convenient manner than the aforementioned geodetic methods. InSAR is capable of detecting ground surface elevation changes with very high precisions (Zebker et al., 1997; Gabriel et al., 1989; Bürgmann et al., 2000). Chen et al. (2000) argued that InSAR is presently the only technology capable of monitoring the deformation of the Earth’s surface in a large area with dense points, quickly and cost-effective, in day and night under all weather conditions.

In this study, we employ InSAR techniques to investigate the land subsidence phenomena in Shanghai. Data from both the European Remote Sensing (ERS) Satellite 1 and 2 (ERS-1/2) and the Japanese Earth Resource Satellite 1 (JERS-1) were used. Results of both qualitative and quantitative mapping of the of the land subsidence phenomenon in Shanghai have been presented. Qualitative mapping of the extent or limits of the subsidence problem was achieved using JERS-1 interferograms over Shanghai from 1992-1998. The quantitative mapping of the subsidence was performed using (i) the DInSAR technique with the L-band JERS-1 SAR data, and (ii) the PSInSAR technique with the C-band ERS-1/2 SAR data.

2. COHERENCE ANALYSIS

Coherence analysis was performed in a section of Shanghai covering the downtown area where the problem of land subsidence is severe in order to assess the behaviour of scatterers in Shanghai over time. The region of interest selected for coherence analysis spans approximately 9 km in azimuth direction and 8 km in range direction. The coherence analysis was also performed to assess which of the SAR data, either the C-band or the L-band, would be suitable for mapping the subsidence phenomena in Shanghai. Figure 2 shows both the region of interest selected for the entire study and coherence analysis from ERS-1 SAR amplitude image of Shanghai acquired on 31 March 1998.

2.1 Data Selection and Processing

Data from both the ERS-1/2 (C-band) and JERS-1 (L-band) SAR systems were used for the analysis. In order to minimize the effect of baseline decorrelation on the final results, only InSAR pairs having ‘small’ normal baselines were selected. In the case of ERS-1/2 SAR data, interferograms having a normal baseline of at most 200m were selected, while a cut-off baseline of 1350m was used for the JERS-1 SAR data. Twenty-seven JERS-1 and 33 ERS-1/2 interferograms were generated for the coherence analysis. The distribution of normal baselines

(B_{\perp}) and temporal baselines (B_t) from the two datasets used for the coherence analysis is presented in Table 1. The total coherence for each InSAR pair was estimated from InSAR processing using the EarthView InSAR v3.1 software. Temporal coherence for each InSAR pair was then estimated by calculating and removing the influence of both the thermal and spatial decorrelations from the total coherence using equation (1) (Zebker and Villasenor, 1992) and individual sensor parameters.

$$\gamma_{temporal} = \gamma_{total} / \left(1 - \frac{|B_{\perp}|}{B_{\perp c}} \right) \left(\frac{1}{1 + SNR^{-1}} \right); \quad B_{\perp} < B_{\perp c} \quad (1)$$

where $\gamma_{temporal}$ = temporal decorrelation
 γ_{total} = overall coherence
 B_{\perp} = the normal baseline
 $B_{\perp c}$ = the critical baseline
 SNR = the signal-to-noise ratio of the SAR sensor.

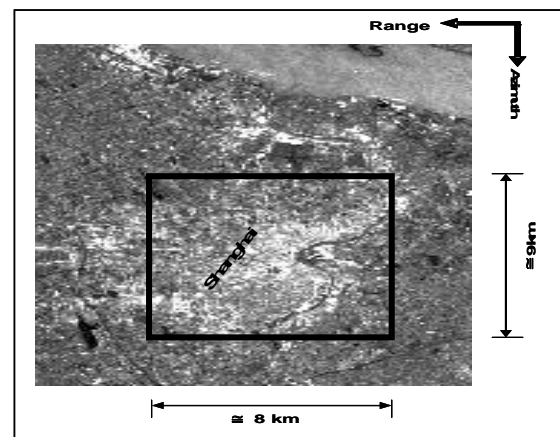


Figure 2. Region selected for both the study and coherence analysis.

Parameter		SAR Sensor	
		ERS-1/2	JERS-1
Normal Baseline, B_{\perp} (m)	Min.	1	1
	Max.	189	1313
	Mean	76	517
	St. dev.	53	363
Temporal Baseline, B_t (days)	Min.	1	44
	Max.	2054	1936
	Mean	890	794
	St. dev.	624	507

Table 1. Distribution of normal and temporal baselines of SAR data used for coherence analysis.

2.2 Results

The result of coherence analysis is presented in Figure 3. It can be seen from the Figure that temporal coherence for both sensors are higher than their respective total coherences. It is also evident from the Figure that JERS-1 SAR interferograms have higher coherence (both total and temporal) than the ERS-1/2 SAR over the study area, despite the longer normal and temporal baselines used in the case of JERS-1 SAR data. It can

be seen that ERS-1/2 SAR data do not maintain good coherence levels after a temporal baseline of 7 months. It is evident from Figure 3 that majority of the interferometric pairs used in this study have coherence levels that fall below the optimum, 0.3.

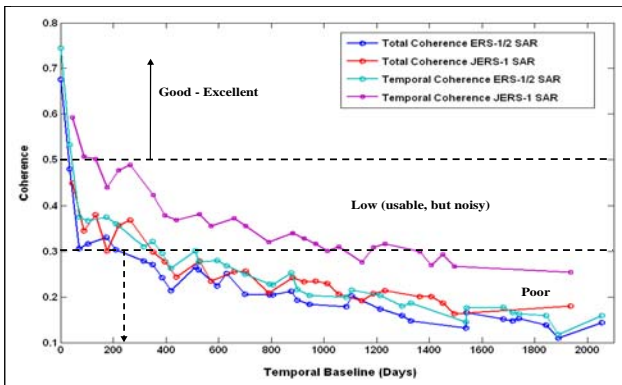


Figure 3. Comparison of coherence between ERS-1/2 and JERS-1 SAR data over Shanghai

3. QUALITATIVE MAPPING OF LAND SUBSIDENCE

In this section, we present the results of using L-band JERS-1 SAR differential interferograms acquired during the period October 1992 to August 1998 to delimit and to track the stages of the land subsidence phenomenon of Shanghai. From the previous section, it was shown that most of the interferograms produced for coherence analysis had their coherence levels falling below the optimum, 0.3. However, they were very useful for qualitative analysis of the land subsidence phenomenon in Shanghai at different stages.

3.1 Data Selection and Processing

The choice of using JERS-1 interferograms over ERS-1/2 is dependant upon the results obtained from coherence analysis performed above. With even longer normal and temporal baselines used in the case of JERS-1 SAR data, they produced reasonably higher levels of coherence than the ERS-1/2 SAR data. That is JERS-1 data makes it possible to use longer normal and temporal baselines to produce suitable interferograms than the ERS-1/2. A total of 20 differential interferograms and 2 DEMs were generated to track the developmental stages of land subsidence in Shanghai. The data has minimum relative temporal baseline of 44 days, maximum relative temporal baseline of 1364 days, minimum relative normal baseline of 2m, and maximum relative normal baseline of 894m. One of the DEMs was used to check the effectiveness of using the other to remove topographic phase from the interferograms generated. Table 2 presents JERS-1 DInSAR pairs used for the qualitative mapping of land subsidence phenomenon in Shanghai. Unlike the ERS-1 and ERS-2 SAR satellites, the JERS-1 has inaccurate orbit information. It is therefore necessary to refine the baseline during data processing to facilitate the removal of flat-earth phase. The flat-earth phases were removed from the interferograms by using a baseline refinement method embedded in the EV-InSAR software, where the normal baseline and the yaw angle are adjusted intuitively and interactively.

No.	Master Image	Slave Image	B _⊥ (m)	B _t (days)
DEM				
1	960810	960923	-894	44
2	960923	961106	-547	44
DInSAR				
1	921002	940906	345	704
2	921002	950301	-418	880
3	921002	950414	442	924
4	921115	930327	815	132
5	921115	960810	781	1364
6	940906	950414	97	220
7	940906	961106	971	792
8	950301	971024	168	968
9	950301	971207	-92	1012
10	950301	980120	862	1056
11	950414	961106	872	572
12	950414	971024	-692	924
13	950414	980120	2	1012
14	961106	980120	-870	440
15	961220	980601	248	528
16	970501	980601	-255	396
17	970910	980828	481	352
18	971024	980715	40	264
19	971207	980715	298	220
20	980120	980715	-655	176

Table 2. JERS-1 interferometric pairs used for qualitative mapping of land subsidence in Shanghai

3.2 Results

Results of the qualitative mapping with JERS-1 SAR data over Shanghai are presented in Figure 4. Three distinct stages of land subsidence were revealed by accumulative subsidence maps shown in Figure 4(a), 4(b) and 4(c). The first stage stretches from October 1992 up to April 1995. The second stage emerged by the end of 1995 and continued to the ending of 1997, where the third stage began to progress. The accumulative land subsidence map of Shanghai produced from other land survey methods is shown in Figure 4(d). It is evident from Figure 4 that the accumulative subsidence maps obtained from InSAR has closed similarities to that produced by other survey methods. However, the extents of the subsidence phenomena have been accurately mapped by the InSAR technique. Some areas marked as stable with land survey methods have been mapped as deforming areas otherwise, and vice versa, by InSAR techniques.

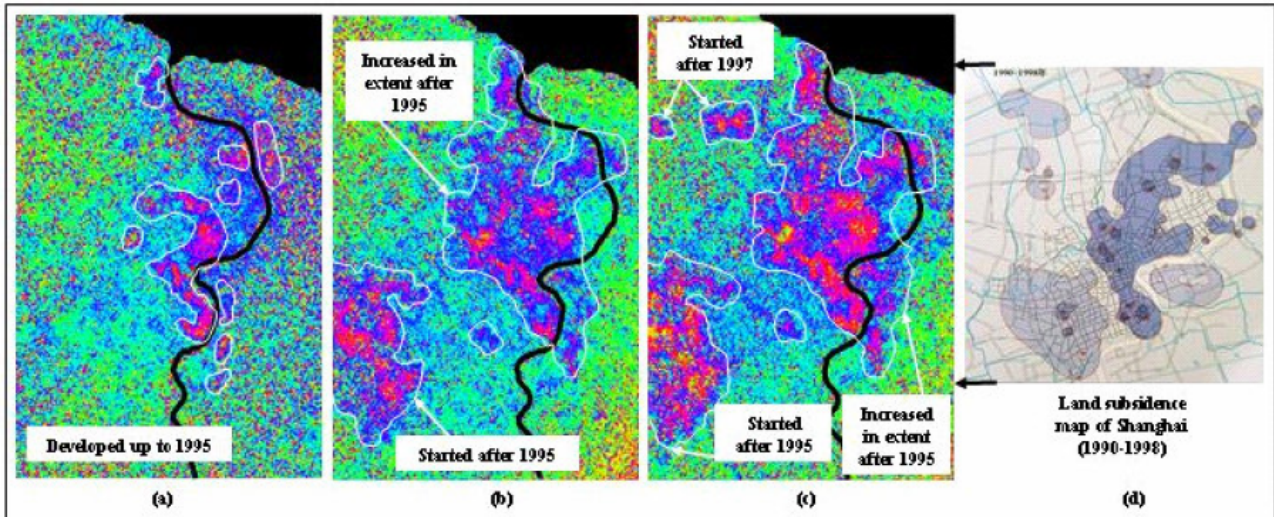


Figure 4. Developmental stages of land subsidence in Shanghai from 1992-1998 mapped by JERS-1 SAR data. (a) Stage 1: accumulative subsidence up to April 1995; (b) Stage 2: accumulative subsidence up to October 1997; (c) Stage 3: accumulative subsidence map up to August 1998; and (d) accumulative subsidence map from 1990-1998 obtained from other survey methods (Source: Zhang et al., 2002).

4. QUANTITATIVE MAPPING OF LAND SUBSIDENCE

This section presents the results of quantitative mapping of the land subsidence phenomenon in Shanghai using both the DInSAR and PSInSAR techniques with datasets acquired by L-band JERS-1 and C-band ERS-1/2 SAR interferometers.

4.1 DInSAR Approach

JERS-1 SAR data acquired over Shanghai in descending orbit, for the period October 1992 to July 1998, were employed in the DInSAR quantitative mapping.

4.1.1 Data Selection and Processing: A total of 8 L-band JERS-1 SAR images covering Shanghai, acquired during the period October 1992 to July 1998 were selected for DInSAR quantitative mapping of land subsidence phenomenon in Shanghai. The data were selected such that differential interferograms generated could form a time series right from the first acquisition to the last.

No.	Master Image	Slave Image	B_{\perp} (m)	B_t (days)
DEM				
1	960810	960923	-894	44
2	960923	961106	-547	44
DInSAR				
1	921002	940906	345	704
2	940906	950414	97	220
3	950414	961106	872	572
4	961106	980120	-870	440
5	980120	980715	-655	176

Table 3. JERS-1 interferometric pairs used for quantitative mapping of land subsidence in Shanghai

The data have minimum relative temporal baseline of 44 days, maximum relative temporal baseline of 704 days, minimum relative normal baseline of 97m, and maximum relative normal baseline of 894m. Three images acquired on 10 August 1996, 9 September 1996 and 6 November 1996 was used to generate 2 different DEMs to remove the effect of topography. In similar manner, the second DEM was used to access the effectiveness of the first regarding the removal of topographic signals from the computed interferograms. A total of 5 differential interferograms were generated with 8 JERS-1 SAR images in Table 3. The flat-earth and the residual phases were removed from the interferograms in similar manner as discussed in Section 3.1.

4.1.2 Results: The final quantitative deformation maps were obtained from post-processing of the DInSAR results with MATLAB. A region covering the downtown area and the surroundings was selected for presentation. This region is made of 1200 pixels in the azimuth direction and 1300 in range direction. Five deformation maps (921002-940906, 940906-950414, 950414-961106, 961106-980120, and 980120-980715), as indicated in Table 3, were stacked to produce an accumulative subsidence map of Shanghai over the period October 1992 to July 1998. Figure 5 presents the 1st, 3rd and the 5th deformation maps obtained for the 5 DInSAR pairs. Figure 6 presents the final accumulative map obtained from the cumulative sum of the 5 deformation maps, as well as the land subsidence map of Shanghai obtained from other survey methods for the period 1990 to 1998.

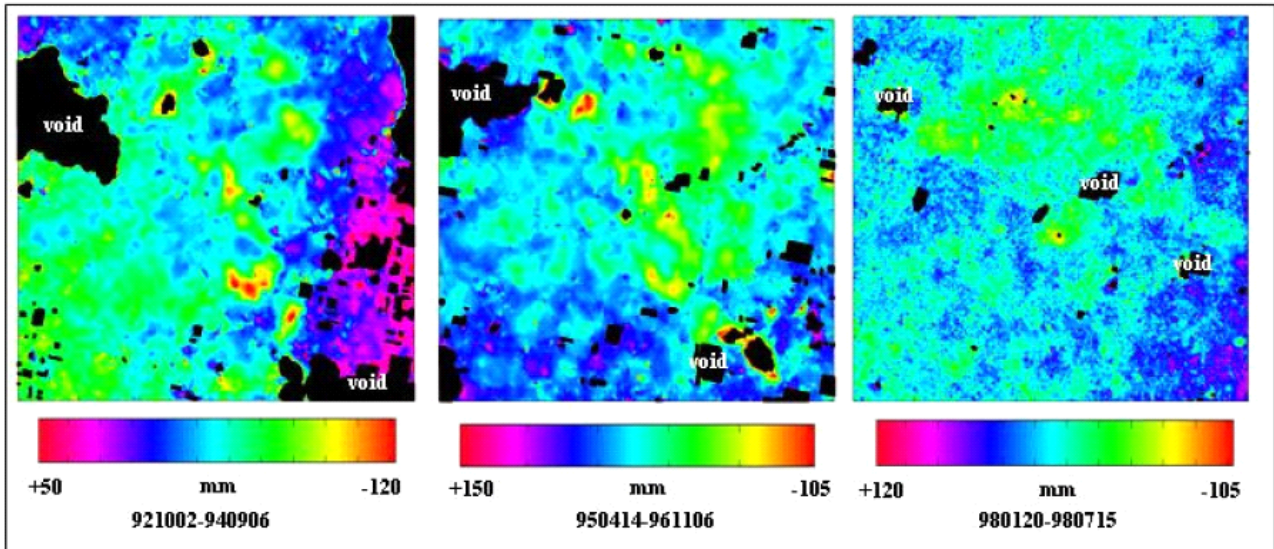


Figure 5. Deformation maps obtained from the 1st, 3rd and 5th DInSAR pairs of the series (see Table 3).

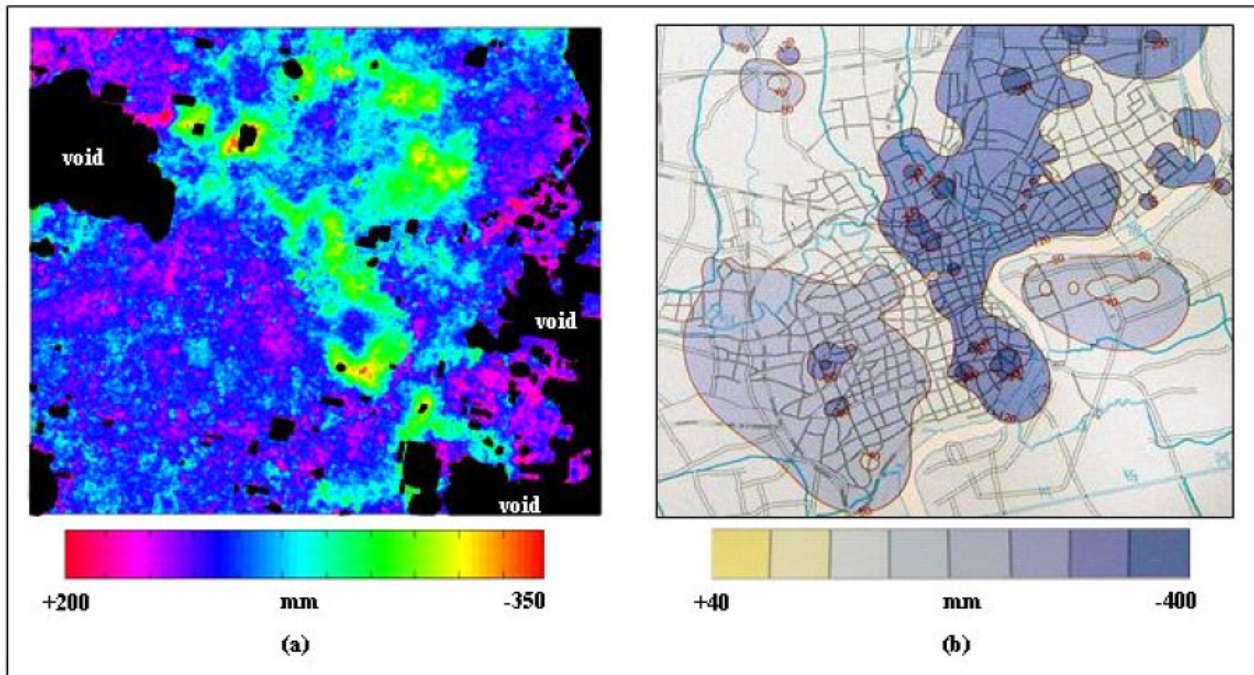


Figure 6. Accumulative land subsidence map of Shanghai: (a) obtained from cumulative sum of 5 deformation maps for the period October 1992 to July 1998; (b) obtained from land surveys for the period 1990 to 1998 (Source: Zhang et al., 2002).

4.2 PSInSAR Approach

PSInSAR quantitative mapping of land subsidence phenomenon in Shanghai was undertaken with datasets acquired by C-band ERS-1/2 interferometers over Shanghai, during the period June 1992 to November 2001.

4.2.1 Data Selection and Processing: A number of factors including normal baselines (B_{\perp}), temporal baselines (B_t) and Doppler centroid variations at the centre swath of SAR scenes (ΔDPC), were taken into consideration during data selection. The common master SAR image was selected based on (1) an image that forms as many as possible interferometric

combinations with others, (2) an image that minimises the dispersion of normal and temporal baselines, and Doppler centroid variations between others, and (3) the date, time and weather conditions during data acquisition. It is expedient to select an image acquired near the centre of the temporal baseline. Based on the above considerations, SAR data acquired on 5 May 1998 was selected as a common master. A 90m resolution C-band Shuttle Radar Topography Mission (SRTM) DEM was used to remove topographic fringes from all the interferometric pairs to yield the differential interferograms. Table 4 presents the ERS-1/2 SAR data processed for the

PSInSAR quantitative mapping of land subsidence phenomenon in Shanghai.

No.	Acq. Date	B_{\perp} (m)	B_t (days)	ΔDPC (Hz)
1	06/06/1992	152	-2159	-306
2	19/09/1992	41	-2054	-269
3	17/04/1993	90	-1844	-284
4	31/07/1993	-9	-1739	-249
5	13/11/1993	-529	-1634	-233
6	10/04/1995	-458	-1121	-229
7	02/10/1995	-44	-946	-273
8	19/02/1996	358	-806	-175
9	20/02/1996	399	-805	75
10	31/03/1998	-516	-35	51
11	05/05/1998	0	0	0
12	20/04/1999	120	350	-37
13	25/05/1999	-145	385	-52
14	16/11/1999	-348	560	17
15	21/12/1999	-398	595	12
16	09/05/2000	357	735	-299
17	13/06/2000	-468	770	238
18	26/09/2000	118	875	21
19	20/11/2001	-141	1295	-646

Table 4. ERS-1/2 SAR data processed for PSInSAR quantitative mapping of land subsidence in Shanghai

4.2.2 Results: Over 22000 PS were extracted, using a temporal coherence threshold of 0.78. The deformation rates obtained fall in the interval -22mm/yr and +5 mm/yr. This value is in agreement with the reported deformation rates over Shanghai during the 1990s (China Daily, 2003b). However, the persistent scatterers depicted regular pattern at some regions in the study area while in some regions the pattern depicted was not easy to interpret. Some reasons suggested for the irregular pattern could be due to the presence of random noise that could not be minimized or removed during PS processing. Figure 7 presents the results of the deformation map obtained after calibration. Figure 8 presents the point profile or deformation history, from 1992 to 2001, of a point selected from Shanghai downtown area. It is evident from the graph that the point experienced a linear subsidence of about 70 mm within the 9.5 years interval.

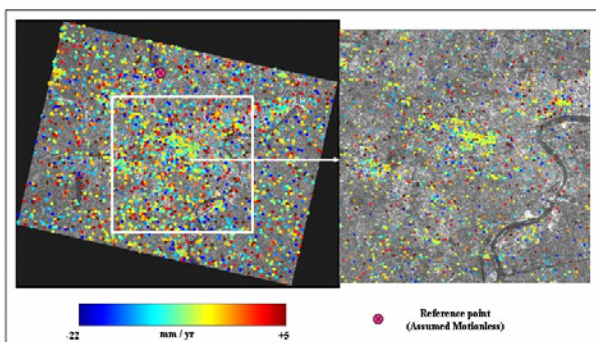


Figure 7. Deformation map obtained from PS processing using C-band ERS-1/2 SAR data over Shanghai for the period 1992 to 2001.

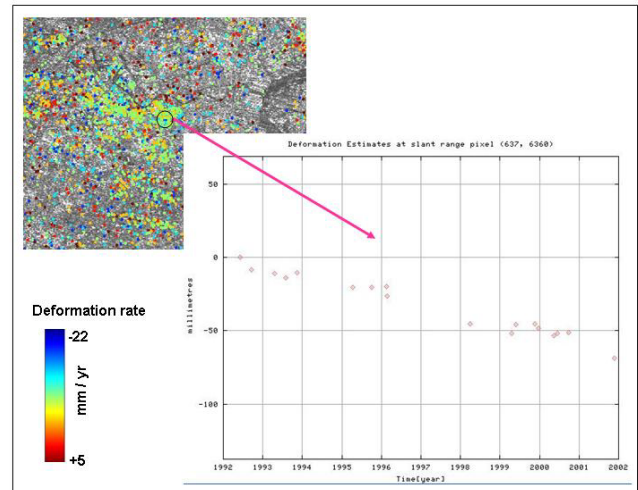


Figure 8. Deformation history of a point in Shanghai downtown area from 1992 to 2001.

5. CONCLUSION

In this paper, we have shown the capability of using InSAR techniques to map land subsidence phenomenon in both qualitative and quantitative terms. DInSAR techniques make it possible to study the extent and pattern of land subsidence phenomenon more efficiently than any other method available today. The problem of loss of coherence in Shanghai has also been demonstrated in this study with both the C-band ERS-1/2 and L-band JERS-1 SAR data. The strength of using the L-band JERS-1 SAR data for mapping low coherence areas such as Shanghai is an important highlight of this study. The result obtained from PSInSAR analysis using the C-band ERS-1/2 SAR data was a bit noisy; nevertheless, it was in agreement with reported annual deformation rates of Shanghai. Also, results obtained from DInSAR analyses using the L-band JERS-1 SAR data were in agreement with the land subsidence maps of Shanghai obtained from other survey methods (see Zhang et al., 2002).

ACKNOWLEDGEMENTS

ERS-1 and ERS-2, and JERS-1 SAR images are copyright © 1992-1998 of European Space Agency (ESA), and Japan Aerospace Exploration Agency (JAXA), respectively, and were provided by the ESA and JAXA. The work was supported by the Research Grants Council of the Hong Kong Special Administrative Region Government (Project No.: PolyU 5157/05E). The first author would like to express his sincere thanks to the Hong Kong Polytechnic University for providing him a studentship to enable him to pursue PhD studies.

REFERENCES

References from Journals:
 Bürgmann, R., Rosen, P.A and Fielding, E.J., 2000. Synthetic aperture radar interferometry to measure Earth's surface topography and its deformation. *Annual Reviews of Earth and Planetary Sciences*, 28, pp. 169-209.

- Chai J.C., Shen, S.L., Zhu, H.H. and Zhang, X.L., 2004. Land subsidence due to groundwater drawdown in Shanghai. *Géotechnique*, 54(2), pp. 143-147.
- Chen, Y.Q., Zhang, G.B., Ding, X.L. and Li, Z.L., 2000. Monitoring Earth surface deformations with InSAR technology: principle and some critical issues. *Journal of Geospatial Engineering*, 2(1), pp. 3-21.
- Damoah-Afari, P., Ding, X.L. and Lu, Z., 2005. Subsidence phenomenon in Shanghai measured with PSInSAR: some preliminary results. *Journal of Geospatial Engineering*, 7(2), pp. 28-38.
- Deng, A.S. and Ju, J.H., 1994. Land subsidence, sinkhole collapse and Earth fissure occurrence and control in China. *Journal of Hydrological Sciences*, 39(3), pp. 245-256.
- Gabriel, A.K., Goldstein, R.M. and Zebker, H.A., 1989. Mapping small elevation changes over large areas: differential radar interferometry. *Journal of Geophysical Research*, 94(B7), pp. 9183-9191.
- Hu, R.L., Yue, Z.Q., Wang, L.C. and Wang, S.J., 2004. Review on current status and challenging issues of land subsidence in China. *Engineering Geology*, 76, pp. 65-77.
- Xue, Y.Q., Zhang, Y., Ye, S.J., Wu, J.C. and Li Q.F. Land subsidence in China. *Environmental Geology*, 2005, 48, 713-720.
- Zebker, H.A., Rosen, P.A. and Hensley, S. Atmospheric effects in interferometric synthetic aperture radar surface deformation and topographic maps. *Journal of Geophysical Research*, 1997, 102(B4), 7547-7563.
- Zebker, H.A. and Villasenor, J., 1992. Decorrelation in interferometric radar echoes. *IEEE Transactions on Geoscience and Remote Sensing*, 30(5), pp. 950-959.
- References from Books:**
- Zhang, A.G., Luo, D.Y., Shen X.G., Lü, L.A., Chen, H.W., Wei, Z.X., Yan, X.X., Fang, Z., and Shi, Y.Q., 2002. *Shanghai Geological Environmental Atlas: Editorial Board* (SGEAEB). Geological Publishing House, Beijing, pp. 130-133.
- References from Other Literature:**
- Gong, S.L., Wu, J.Z. and Yan, X.X., 2005. Analysis of land subsidence due to construction engineering in soft soil region of Shanghai. In: *Proceedings of the 7th International Symposium on Land Subsidence*, Shanghai, China, Vol. 1, pp. 82-87.
- Yang, G.F., Wei, Z.X. and Huang, C.S., 2005. Advances and challenge in research on land subsidence in China. In: *Proceedings of the 7th International Symposium on Land Subsidence*, Shanghai, China, Vol. 1, pp. 3-9.
- Zhang, A.G. and Wei, Z.X., 2005. Prevention and cure with Shanghai land subsidence and city sustaining development. In: *Proceedings of the 7th International Symposium on Land Subsidence*, Shanghai, China, Vol. 1, pp. 10-17.
- References from Other Literature:**
- China Daily, 2003a. Shanghai puts up a fight to stop sinking. *China Daily*, 16 July 2003 Edition. http://www2.chinadaily.com.cn/en/doc/2003-07/16/content_245660.htm (accessed April 2003).
- China Daily, 2003b. Cites Sinking due to Excessive Pumping of Groundwater. *China Daily, Hong Kong Edition*, 11 December 2003. http://www.chinadaily.com.cn/en/doc/2003-12/11/content_289290.htm (accessed: January 2004)
- Shi, L.X. and Bao, M.F., 1994. Case History No. 9.2 – Shanghai, China. In Poland, J.F. ed. *Guidebook to studies of land subsidence due to groundwater withdrawal*, UNESCO, Paris. <http://wwwrcamn.wr.usgs.gov/rgws/Unesco/PDF-Chapters/Chapter9-2.pdf>. (accessed April 2003)

